Renewable Energy 251 (2025) 123397

Contents lists available at ScienceDirect

Renewable Energy

journal homepage: www.elsevier.com/locate/renene

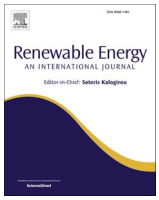

Energy assessment of thermal solar-powered district heating and cooling networks for a cluster of buildings in Mediterranean climate

Tancredi Testasecca *, Pietro Catrini, Maurizio La Villetta, Marco Beccali, Antonio Piacentino

Department of Engineering, Università degli Studi di Palermo, Palermo, 90128, Italy

ARTICLE INFO

Keywords:
District heating and cooling
Solar cooling systems
Dynamic simulation
Ring network
Solar thermal energy

ABSTRACT

The urgent need to cut carbon dioxide emissions in buildings is pushing towards efficient, eco-friendly solutions for meeting heating and cooling demands such as renewable-based district heating and cooling networks. In this context, very few studies have investigated the potential of these technologies in Southern Mediterranean regions, characterized by predominant cooling demands and large availability of renewable energies. In this respect, this work proposes an energy analysis of modern district networks composed of solar collectors, absorption chillers, heat pumps, and thermal energy storage, serving a cluster of buildings in Southern Italy. Using a dynamic model for a double-loop ring network and solar plant developed in Transient System Simulation tool, different scenarios are simulated. Specifically, a baseline scenario, where thermal demand is met individually, is compared with low-temperature (60–85 °C) and ultra-low-temperature (7–20 °C) networks. An examination of primary energy consumption, carbon dioxide emissions, temperatures, and pressure within the network reveals that the proposed improvement scenarios lead to energy savings respectively from 62% to 82% compared to autonomous heating and cooling systems. Additionally, ultra-low temperature district reduces heat losses in pipes by 67.4% compared to low-temperature operation. However, the energy needed by booster heat pumps in the case of an ultra-low temperature network leads to higher primary energy consumption of a factor of 2.1 compared to the case of a low-temperature network. The present work provides a picture of the energy and environmental benefits achievable by these innovative systems in cooling-dominated areas, underlying the need for future research for spreading these systems in these regions.

1. Introduction

According to the International Energy Agency (IEA) [1], in 2022, 80 % of direct carbon dioxide (CO_2) emissions from buildings were attributed to space heating (SH) and domestic hot water (DHW), with over 60 % of this demand being met by fossil fuels. Large-scale implementation of efficient, low-carbon heating technologies combined with the improvement of building envelopes is increasingly necessary to achieve the Net Zero Emissions scenario goals by 2050 [1].

District Heating and Cooling Networks (DHCNs) represent one of the most promising technologies for transitioning toward more sustainable heat production in buildings [2]. District Heating Network (DHN), unlike individual heat production, relies on mostly centralized thermal energy production to increase energy efficiency and reduce the use of fossil fuels [3]. These networks, generally powered by cogeneration plants or industrial boilers, thanks to recent developments, could allow the integration of Renewable Energy Sources (RESs) [4]. The evolution of this technology is identified through five generations, corresponding to significant changes. Currently, many DHNs distribute heat through pipes as pressurized water at supply temperatures above 80 °C (being classified as 3rd generation DHNs), with thermal losses ranging from 10% to 30% [5].

In recent years, the evolution towards Fourth Generation District Heating Networks (4GDHNs) has been driven by the decarbonization goal and has featured a further decrease in the water supply temperature, below 70 °C [6]. The lower supply temperature reduces heat losses through the network and allows for the integration of heat from RES and waste heat from industrial processes [7]. Simultaneously,

This article is part of a special issue entitled: SDEWES2024 published in Renewable Energy.

* Corresponding author.
E-mail addresses: tancredi.testasecca@unipa.it (T. Testasecca), pietro.catrini@unipa.it (P. Catrini), maurizio.lavilletta@unipa.it (M. La Villetta), marco.beccali@unipa.it (M. Beccali), antonio.piacentino@unipa.it (A. Piacentino).

https://doi.org/10.1016/j.renene.2025.123397
Received 30 November 2024; Received in revised form 6 March 2025; Accepted 7 May 2025
Available online 8 May 2025

Fifth-Generation District Heating Networks (5GDHNs) that use water at temperatures close to that of the air or ground, with maximum values below 30 °C are also being developed [8].

5GDHNs were developed to overcome some limits of the 4GDHN, i.e., further reducing the water supply and the thermal losses of the plant, fully exploiting low-temperature heat sources, and meeting the cooling and heating demands of users simultaneously. The ultra-low temperature requires Vapor Compression Heat Pump (HP) at the user's substation to produce heat at the desired temperature [9]. However, decentralized HPs allow the connection between the electrical grid and DHNs to create smart thermal grids with power-to-heat technologies [10].

Among RES-based DHN technologies, Solar District Heating (SDH) systems are a promising solution for decarbonizing the building sector [11]. Denmark is a European leader in this field [12], with one of the first SDH networks installed in Marstal, featuring a 75,000 m^3 storage capacity and over 30,000 m^2 of solar collectors [13]. By the end of 2021, 299 large SDH plants were operational with an installed capacity of 1645 MW_{th} [14]. However, these systems remain very uncommon in Southern Mediterranean regions, where high cooling demand has limited their adoption despite abundant solar energy.

Integrating SDH with Solar Cooling (SC) technologies in this area could enhance their viability. In SC systems, thermal energy from solar collectors drives absorption chillers (ABSs) to produce cooling [15]. Despite absorption machines having limited performance, they are particularly interesting when coupled with thermal collectors, allowing them to reduce non-renewable Primary Energy (PE) consumption [16]. While single-stage ABSs are predominantly used due to the lower temperatures of heat generated by RESs [17,18], recent studies have shown that SC can also be achieved with double-effect ABSs utilizing concentrating solar collectors [19]. Additionally, SC has been explored through the diffusion-absorption refrigeration cycle, which is characterized by a thermally driven bubble pump powered by evacuated tube solar collectors [20,21].

To address the intermittent nature of solar energy, large thermal energy storage (TES), or seasonal TES, allows to store thermal energy by centralized solar plants [22]. Among these, Pit Thermal Energy Storages (PTESs), are mainly used for applications where there is a need to store a large amount of heat from solar plants.

The interest in solar heating and cooling programs is also confirmed by the development of different tasks by the IEA such as Task 65 and Task 68 [23]. In this framework, the IEA's "Sustainable District Heating Guidelines" [24] stated that flat plate and evacuated tube solar collectors are the most diffuse type of solar source in SC, and 80% by 2015 of solar thermal cooling systems were installed in Europe.

1.1. Literature review

In the current literature, there are limited applications of solar-assisted DHCNs in Mediterranean regions. Specifically, very few examples pertain to Mediterranean countries such as Italy, Greece, or Spain. Recent research and applications are increasingly focusing on DHNs coupled with solar collectors. The primary motivation lies in the significant potential to reduce reliance on fossil fuels, as demonstrated by real-world applications such as the Marstal Solar-powered DHN [13]. Furthermore, studies on both 4GDHNs and 5GDHNs are being published, and the advantages of powering such novel DHNs by RES have been extensively documented, particularly in Northern European countries such as Denmark [25], Germany, and the Netherlands [26].

Recent attention is being given to the application of solar-assisted DHCNs in Mediterranean countries. In this context, Calise et al. [27,28] presented comparative thermoeconomic studies of 4GDHNs and 5GDHNs in Spain. In [27], the authors used Transient System Simulation Tool (TRNSYS) to model a DHN serving a residential district in Madrid powered by a large photovoltaic (PV) plant, water-to-water (W/W) HPs, and ground-source HPs, achieving up to 98% reductions in operational emissions in the most favorable scenarios. In Ref. [28], a 4GDHN for a large shopping mall was replaced with a 5GDHN consisting of two neutral-temperature rings that allowed users to exchange heat via W/W HPs. This configuration, driven by a PV plant, achieved PE savings of 89% and a simple payback time of 14.2 years, despite an investment cost of 11.2 M€.

Other studies have proposed solar-driven DHNs for new urban developments or retrofitting existing networks. For instance, De Rosa et al. [29] investigated the impact of various energy policies for a new 3.5 km^2 district in Madrid. This scenario featured a DHCN with multiple loops, ground-source HPs, and high PV penetration. Results showed a 66% reduction in non-renewable PE consumption and a significant decrease in peak electricity demand, albeit with high investment costs. Mugnini et al. [30] studied retrofitting strategies, such as installing high-temperature HPs exchanging heat with the network, for a DHN located in Central Italy using dynamic simulations trained on real-world data. Leveraging surplus electricity from an extensive PV installation, Natural Gas (NG) consumption was reduced by 13.3%. Xu et al. [31] proposed a 2.5 MW air-to-water HP coupled with 6355 m^2 of solar thermal collectors and a storage tank was used to reduce boiler operation hours in a real DHN in the Danish city of Ørum. The proposed operational strategies for the heat production plant resulted in a reduction of the CO_2 emissions factor from 192 kg_{CO2}/MWh to 74 kg_{CO2}/MWh.

Focusing on solar thermal systems, Ghirardi et al. [32] compared hot water provision with ABS and chilled water provision by single ABS driven by heat from parabolic-through collectors. In the network considered, located in the United Arab Emirates, with 24 MW of cooling load peak, heat losses related to hot water provision led to higher heat losses compared to cooling provision. Different SC configurations, including PV, Photovoltaic Thermal (PVT) and thermal collectors, as well as electrical and ABSs were investigated by Ismaen et al. [33]. Hybrid and thermal solar driven scenarios succeed in reducing environmental impact at least 43.8 % and increase solar fraction up to 94.7% in PVT case. Finally, in [34] solar parabolic trough collectors and DH supplied hot water to an ABS for a hospital located in Denmark. Considering summer period, thanks to the provided system 85% of emissions were reduced by the system considered with a payback period of only 7.5 years.

1.2. Research gaps and paper contributions

The referenced studies demonstrate that energy benefits could be achieved by incorporating solar energy into DHCNs. Indeed, all of them, sometimes supported by thermo-economic analyses, consistently report reductions in dependency on non-renewable energy sources, emissions, and operational costs for providing SH and DHW [27,28]. However, the following gaps could be identified:

- No comparative energy analyses have explored the benefits of novel DHCNs in Southern Mediterranean regions are available. Such studies could support the spread of these technologies in cooling-dominated areas with abundant solar energy. Additionally, they could help identify the optimal mix of renewable energy technologies, suitable operating strategies, and the necessity to integrate energy storage systems.
- The integration of SC via DHNs in Southern Europe countries has not been extensively studied. These regions typically experience low heating demand in winter and high cooling demand in summer (which is also expected to increase due to climate change). The large availability of solar radiation during summer could promote the adoption of SC systems. Additionally, utilizing the district network to distribute heat from decentralized solar plants to drive SC technologies at the user level could encourage the adoption of DHNs in climates where they are not yet widely implemented.

- Few studies have compared pumping energy consumption and the hydraulic performance of low- and ultra-low-temperature DHNs. Existing research lacks a comprehensive analysis of pressure profiles and pumping energy requirements in such networks. Since these networks operate with significantly different flow rates and supply-return temperature differentials, further research is needed to assess their impact on overall system efficiency.
- Finally, dynamic analyses describing the operation of novel DHN generations coupled with solar systems are lacking, particularly from both network and plant perspectives. Monitoring the effect of solar energy variations on the supplied water temperature and the amount of thermal energy stored could help develop new cost-effective operating strategies.

To address these gaps, this paper presents an energy analysis of innovative DHCNs supplied by a solar plant and serving a cluster of buildings located in Southern Italy. Specifically, based on prior research by the authors [35] which examined the benefits of 4GDHNs compared to third-generation networks through dynamic simulations, this study develops a novel model that includes booster HPs, and centralized solar plants with storage using TRNSYS software [36]. This tool, offering accurate models for complex renewable energy systems, is widely accepted in the literature and has thus far formed the basis for a great number of studies [27,28,37–40]. A key innovation of this model is the integration of a detailed solar plant, including a large solar collector field, a PTES system, and industrial ABSs. The main plant is also equipped with auxiliary boilers and auxiliary air-cooled chillers. The study evaluates two alternatives for providing cooling energy to an eight-user cluster. The first one involves the direct supply of chilled water produced by solar-fed ABSs. The second involves indirect supply through hot water-fired ABSs installed at each user substation. Similarly, two strategies are compared: direct supply of hot water (up to 60 °C in winter) versus the use of warm water (at 20 °C) combined with HPs at user substations. Dynamic simulations will provide insights into network and plant operations, analyzing energy consumption and variation in CO_2 emissions. The following contribution can be then identified:

- A comparative analysis of PE savings and reduction in CO_2 emissions achieved by two solar-powered DHNs in cooling-dominated zones is carried out. The analysis aims at identifying the potential of innovative DHNs supplied with solar energy in decarbonizing the building sectors, in a context where the prevalent cooling demand has limited so far, the spread of this technology. Meantime, benefits and drawbacks will be identified. For instance, the additional electricity consumption due to booster HPs in the case of ultra-low-temperature DHNs will be compared to the additional natural gas consumed in the case of low-temperature DHNs.
- Two alternative ways for meeting the heating and cooling demand using thermal energy from a centralized solar-powered are compared to highlight which one outperforms in terms of solar energy exploitation, and reduction in PE consumption for heating and cooling.
- The importance of dynamic analysis in monitoring the operation of this system is evidenced, especially in the case of intermittent energy sources. The amount of solar energy stored temperature and pressure profile are evaluated. A yearly and hourly comparison of low-temperature and ultra-low-temperature DHN operations is conducted, evaluating pressure drops, pumping energy, and heat losses.

2. Materials and method

In this section, the overall system layout and operational strategy are first presented. Then, the modeling of the solar loop and DHNs is shown.

2.1. Scheme of the solar loop and district heating network

Fig. 1a-b shows two schemes of the investigated solar-powered network, when providing hot and chilled water, respectively. It must be noted both schemes represent a comprehensive and redundant superstructure that includes all the components that will be used in the different scenarios.

In both schemes, the pump of the solar loop is activated during the daytime, only if the outlet temperature of the water outside the solar field is higher than the inlet water temperature. In addition, the hot water produced in periods of low heating demand and high solar radiation is stored in a PTES used as seasonal energy storage. PTESs are dug-out pits, lined with a membrane and a layer of insulation, and filled with water at operating temperatures typically between 30 °C and 90 °C [41]. The solar loop could provide hot water at different temperatures (see Fig. 1a) or chilled water (see Fig. 1b).

In the case of “Hot Water Provision”, the district directly interacts with the PTES in the “Solar Loop” section. Specifically, the cold water returning from the district is heated up in the PTES, and, if the exiting temperature is not compatible with the supply water temperature setpoint of the DHN, a fraction of the flow rate is further heated up in an auxiliary boiler. Conversely, if the temperature of the water exiting the PTES is higher than the setpoint, a thermostatic valve will mix this flow with the flow from the return side of the network to achieve the desired temperature.

In the case of “Chilled Water Provision” (see Fig. 1b), the Solar Loop will supply chilled water to the DHN supply ring. The water flow returning from the district interacts firstly with the ABS, which will cool down the water. Note that the ABS is driven by heat produced in the solar plant and stored in the PTES. If there is no sufficient heat to cool down the water at the desired temperature setpoint, a thermostatic valve will send the flow toward an industrial auxiliary air-cooled chiller. To remove heat from the condenser of the ABS, an open-circuit cooling tower was also modeled. It must be noted that this mode was only used in one of the scenarios considered in this study.

Regarding the DHN, a double-ring model was adopted. Such a configuration was already studied by the authors [35], and it was found to be promising in the presence of prosumers. In case of consumption, the hot or cool water from the supply side passes, using diverter valves, through the user substation and finally gets injected into the return side.

2.2. Modeling of the solar loop

The modeling of the solar loop was developed in TRNSYS [36]. The scheme of the model used for chilled water provision is represented in Fig. 2. Solar collectors were modeled through Type 71 – Evacuated Tube Collector – which required several input parameters such as ambient temperature, total radiation incident on the panel surface, solar azimuth and zenith angles, and the inclination and azimuth angle of the panels. These data were read from the meteorological dataset by using Type 15 – Weather Data Processor. The pump of the solar plant was modeled through Type 3d – Single Pump model, controlled by a calculator that allows its operation when the fluid temperature exiting the plant is higher than the fluid temperature entering. The PTES system was modeled through Type 4 – Stratified Storage Tank, simulating the behavior of a sensible energy storage tank filled with a fluid, water in this case. The thermal stratification is modeled by assuming the tank consists of 6 segments of equal volume mixed and filled with fluid from the solar plant. The outside boundary is the temperature of the ground available through the Weather Data Processor. The transmittance of the walls of the PTES was calculated considering a concrete wall insulated with 1 m of EPS as recommended in [42]. In both the heating and cooling seasons, the hot water from the solar field directly fed the PTES from one side. During the heating period, the heat carrier fluid exiting the storage is supplied directly to the DHN. In the cooling period, the fluid can either be sent to the ABSs installed at each user’s location or

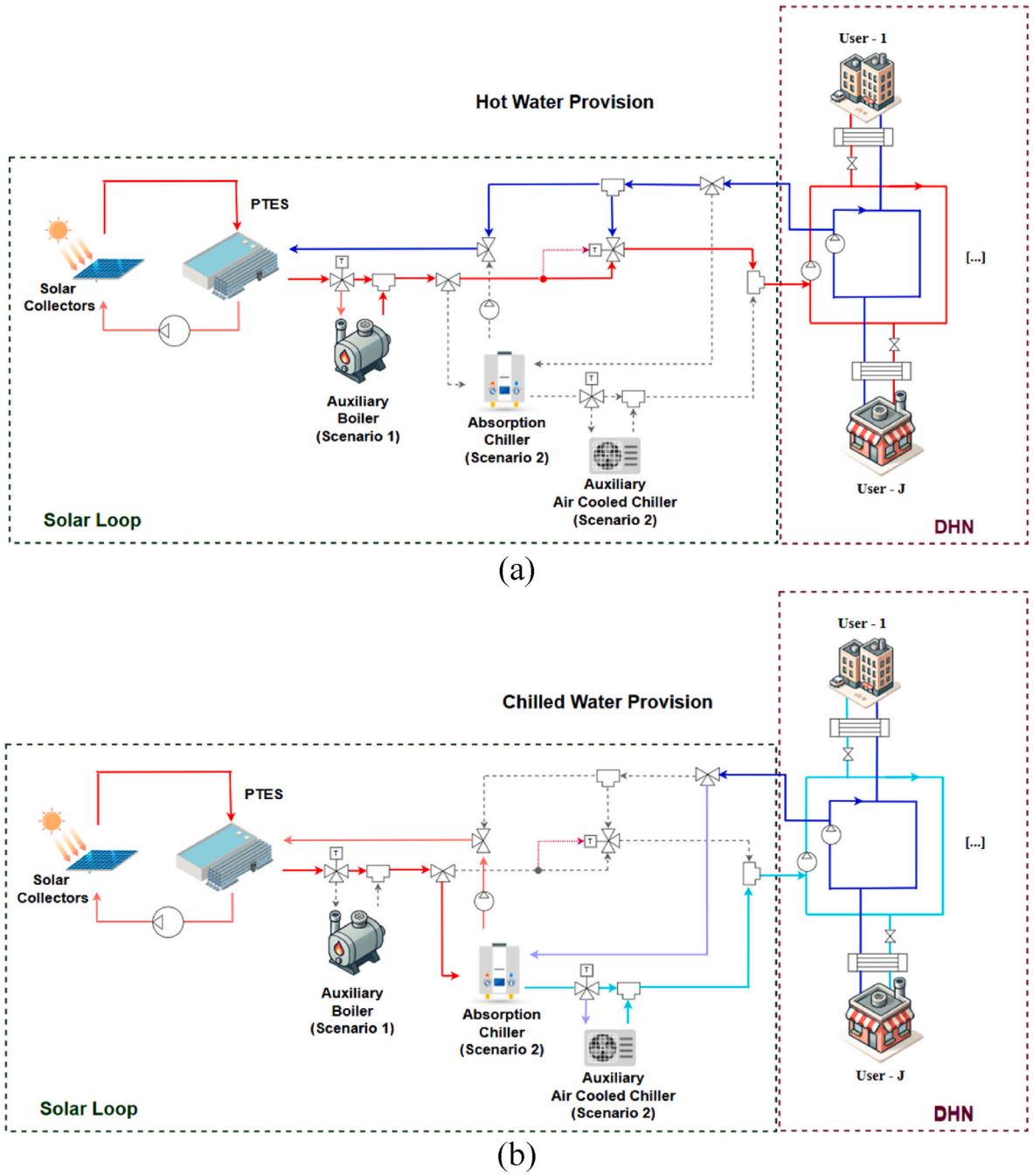

Fig. 1. Simplified schemes of the solar loop and DHN: (a) "hot water provision to the DHN" and (b) "chilled water provision to the DHN".

used to power a central ABS to produce the chilled fluid that feeds the network. If the temperature of the fluid from the storage is lower than the setpoint, an auxiliary heater, simulating the boiler and modeled using Type 6 - Auxiliary Heater and a calculator, is employed to heat the fluid to the desired temperature. Lastly, a thermostatic valve (Type 11 - Tempering Valve) is used to ensure the correct supply temperature by mixing cold water from the DHN with hot water from the storage.

In the case of direct provision of chilled water to the DHN (see Fig. 1b), a centralized ABS is used which directly supplies cold water at 7 °C to network. A macro for this chiller, including calculators and Type 581 - Data Interpolator, was developed to improve the functioning of Type 107 - Single Effect Absorption Chiller. This model requires as inputs the temperature and flow rate of: the ABS's supply fluid, coming from the storage; the fluid to be cooled, coming from the network return piping; the fluid that removes heat from the ABS, necessary for its proper operation. The main equations included in the new macro, are based on Type 107 basic equation as detailed in [43].

As for Type 107, the amount of heat $\dot{Q}_{set}$ that must be removed from the fluid to be cooled from the inlet temperature $T_{\mathrm{ch,in}}$ to the setpoint temperature $T_{\mathrm{ch,set}}$ is described by Eq. (1) [44]:

$$\dot{Q}_{set} = \dot{m}_{ch} c_w \left(T_{\mathrm{ch,in}} - T_{\mathrm{ch,set}}\right) \tag{1}$$

Where $\dot{m}_{ch}$ is the chilled water flow rate, and c_w is the specific heat of the water.

The minimum generator temperature, contingent upon the desired chilled water temperature, set to 7 °C, was first determined based on [45] which is the datasheet of a single-stage LiBr-Water ABS. Knowing the value of this temperature, it is possible to calculate the maximum theoretical amount of heat extractable from the fluid feeding the

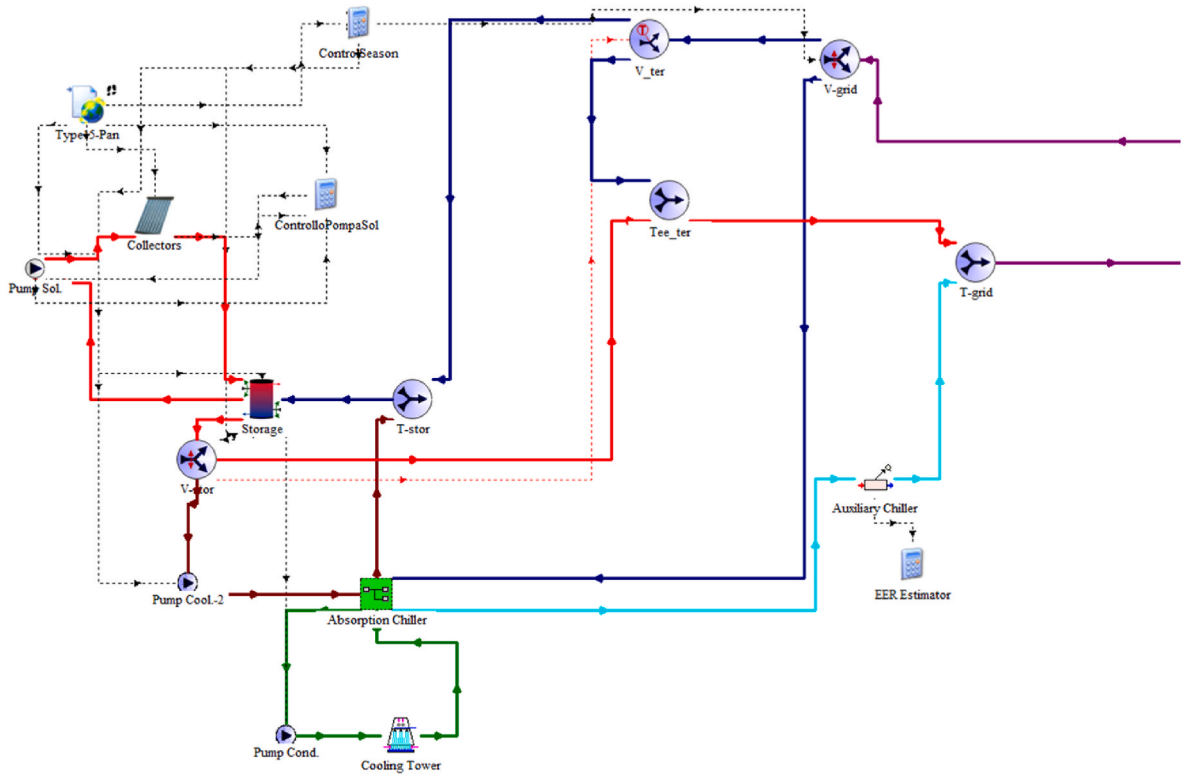

Fig. 2. Modeling of the Solar Loop developed in TRNSYS for chilled water provision.

generator $\dot{Q}_{gen}$ through Eq. (2):

$$\dot{Q}_{gen} = \dot{m}_{gen} c_w \left(T_{\text{gen,in}} - T_{\text{gen,set}}\right) \tag{2}$$

Where $T_{\text{gen,in}}$ is the temperature of the hot fluid entering the chiller, $T_{\text{gen,set}}$ is the minimum temperature of the hot fluid compatible with the chiller operation, and $\dot{m}_{gen}$ is the flow rate of the fluid feeding the generator.

The Coefficient of Performance COP_{ABS} of the ABS is estimated using performance curves available in [45] by knowing the temperatures of entering fluids(chilled water, condenser water and hot water) using Type 581 - Data Interpolator. Having obtained COP_{ABS} and the amount of heat $\dot{Q}_{gen}$, it is possible to calculate the maximum energy removable to the network side fluid $\dot{Q}_{ch,max}$ using Eq. (3):

$$\dot{Q}_{ch,max} = \dot{Q}_{\text{gen}} \cdot COP_{\text{ABS}} \tag{3}$$

Once known the rated capacity of the machine $\dot{Q}_{rated}$ (depending on condenser and generator water temperature), $\dot{Q}_{ch,max}$, and $\dot{Q}_{set}$, the amount of heat removed from the fluid to be chilled will be the minimum of the three quantities. This approach guarantees that the heat removed will always be lower equal than $\dot{Q}_{\text{gen}}$, simulating a partial bypass of the flow rate that would enter the chiller. However, to guarantee the chilled water provision, an auxiliary air-cooled chiller was included and simulated using Type 92 - Auxiliary Cooling Device considering the Energy Efficiency Ratio (EER) of an industrial air-cooled chiller [46]. Finally, to remove the heat from the ABS condenser, an open-loop cooling tower was modeled through Type 51-Cooling Tower.

In detail, COP_{HP} was calculated as shown in Equation (4). COP_{ABS}, see Equation (5), was used for estimating HP efficiency.

$$COP_{HP} = \frac{\dot{Q}_{cond}}{\dot{W}_{el}} \tag{4}$$

$$COP_{ABS} = \frac{\dot{Q}_{ev}}{\dot{Q}_{gen}} \tag{5}$$

Equation (4) represents the COP of the HP COP_{HP}, which is defined as the ratio between the heat delivered at the condenser $\dot{Q}_{cond}$ and the electrical power input $\dot{W}_{el}$. Equation (5) defines the COP of the absorption chiller COP_{ABS}, calculated as the ratio of the cooling capacity at the evaporator $\dot{Q}_{ev}$ to the thermal power required at the generator $\dot{Q}_{gen}$. The electrical power in input to the absorber was assumed negligible compared to the other quantities.

2.3. Modeling of the District Heating Networks

The DHN consists of a ringshaped network, which includes two rings: one for the supply and one for return. Unlike traditional networks, where the return line starts from the last user and returns to the central plant, in this case, both lines start directly from the thermal plant and return to it [47]. The ring network also lends itself better to the connection of potential prosumers as it is more challenging for flow reversals to occur. The DHN was also modeled in TRNSYS (see Fig. 3), and it is mainly composed of six Types, found at each user node, and within the user substations macro. Specifically, Type 11f - Controlled Diverter Valve: used in the supply piping to divert the flow requested by the consumer (or produced by the producer) from the flow that continues to circulate in the network; Type 11h - Tee Piece: the piece used in the return piping to merge two flows, the one circulating in the pipe and the one exiting the user, into a single flow; Type 9e - Data Reader: it reads an external file to import user demands; Type 65a - Online Plotter with File: it is used to obtain the output data both graphically and in document form to analyze in a spreadsheet; Type 31 - Pipe/Duct, used to simulate the heat losses with the ground, and Type 496 - Hydraulic Pipe which was previously developed in [35] for calculating pressure drops. In this work, the supply ring is used to provide hot water, in case of the heating period or cooling period when ABSs are in the user substation,

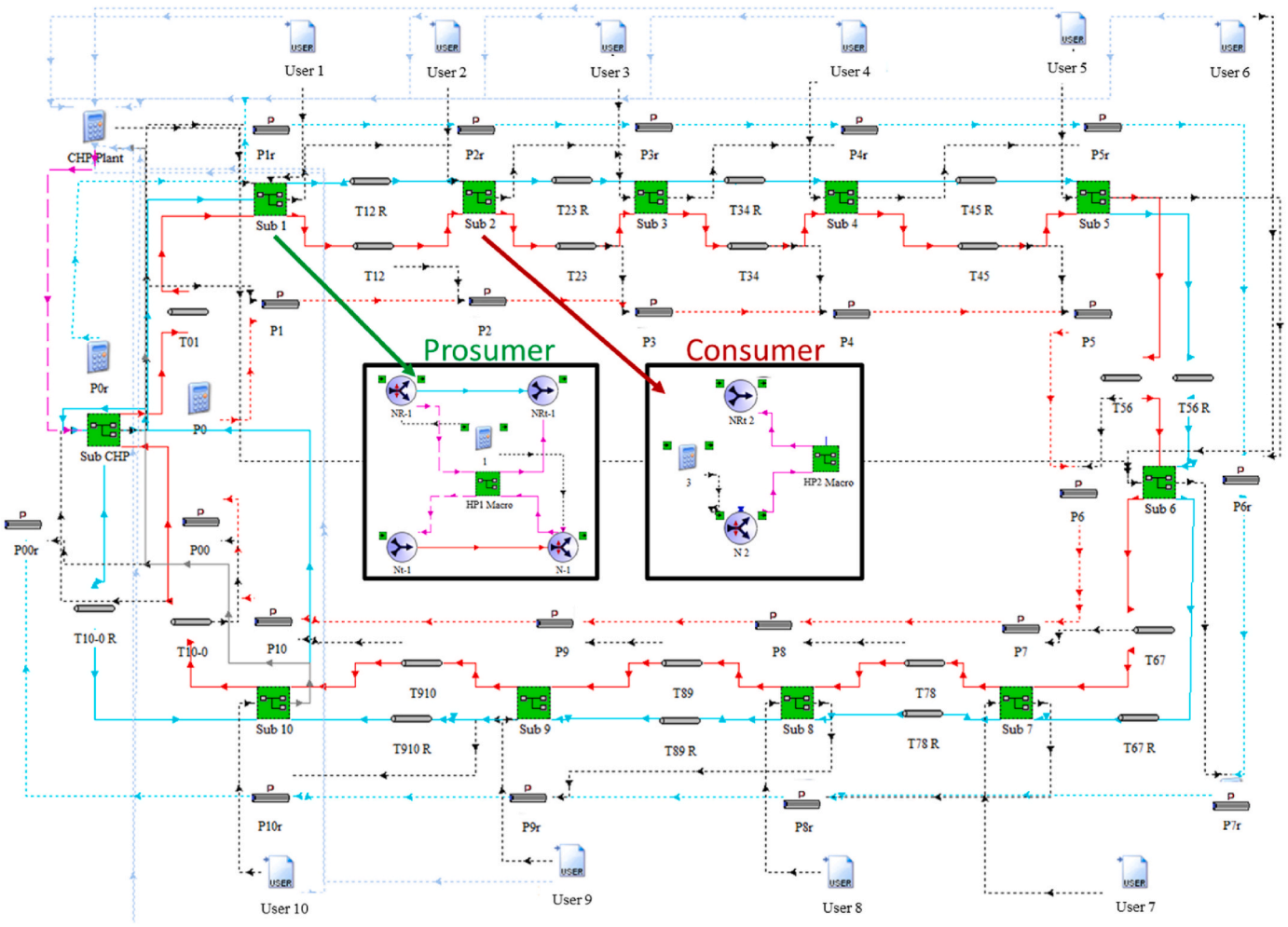

Fig. 3. A 10 User-Prosumer DHN model in TRNSYS.

and chilled water in cases of direct cooling provision.

As previously mentioned, in a 5GDHN, every user usually installs a booster HP within its substation. This is necessary to upgrade the temperature level of the heat from the network to the level required by the local heating system. This possibility was accounted for in this model, and a W/W type HP interfacing with the network (as a source) and the user was included in the user substation. For this reason, the model proposed in [35] was improved. A macro was developed to simulate the behavior of the W/W inverter HP based on the performance curves available in the literature [48] and manufacturer catalogs [49]. The TRNSYS macro for the substation, shown previously in Fig. 3, is expanded and detailed in Fig. 4. For operation in heating mode, the study by Hüsing et al. [48] was considered for calculating the Coefficient of Performance (COP) of an inverter HP. Using Type 581 - Data Interpolator, based on the required power, the system will operate at a different frequency and finally, the COP is calculated also considering the evaporator inlet temperature and condenser outlet temperature. The obtained coefficients of performance, the energy required by the user, the temperature, and the flow rate on the source side are set as input into the calculator named "Exchanger", which calculates the temperature of the fluid exiting the HP and sent to the return ring of the DHN [50]. The flow rate coming from the supply side, regulated by "User" calculator through the User-S valve, goes to the HP macro. Based on the user demand, the "Exchanger" calculator will calculate the outlet condition of

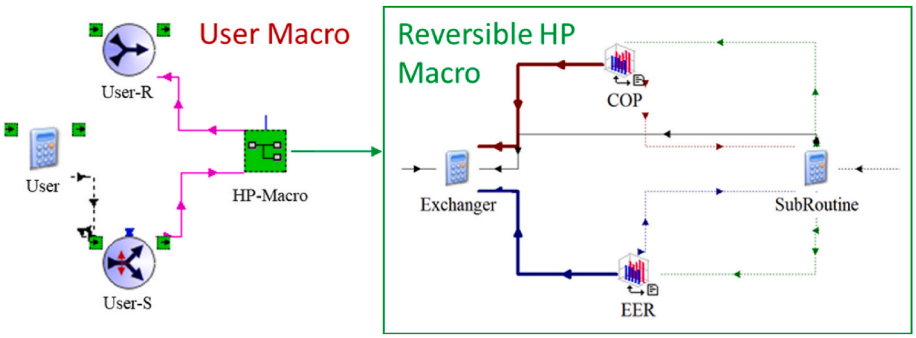

Fig. 4. Macro of the fifth-generation user substation.

the fluid. Finally, the flow rate is injected to the return side using the tee "User-R".

Before ending it is worth stressing that the whole system is difficult to be directly validated, due to high capital costs, and due to the low diffusion of this system. However, the modeling of each component, such as pipes, HPs, and valves has been validated individually [43] by using experimental data or literature making the model of the system inherently reliable.

3. Case study

First, a description of the cluster is provided, along with insights into the climate conditions of the selected locality. Next, details on the investigated scenarios and the design of the solar loop and DHN are provided. Finally, the energy and environmental indicators are introduced.

3.1. Description of the cluster of buildings

The cluster is made up of eight users located in Palermo (Southern Italy). Fig. 5 shows a representation. Specifically, clockwise: a medium-sized office, a group of three high-rise apartments, a hospital, a supermarket, 8 mid-rise apartments, a primary school, a high-density office, and 4 high-rise apartments.

Regarding data on weather conditions and solar irradiation for Palermo, the climate data available in [51] was selected. In detail, Fig. 6 shows dry bulb temperature T_{dry} and Relative Humidity (RH) profiles for Palermo and in Fig. 7, values of global solar irradiation on a horizontal plane are represented.

The hourly heating and cooling demands of the big office, hotel, and hospital were estimated in a previous study by some of the authors [52]. For the other buildings in the cluster, demands were obtained through simulations conducted using EnergyPlus [53], based on building archetypes described in [54]. Specifically, the remaining buildings were customized and revised to align with Palermo's climate and building categories, following Italian regulations as detailed in [47].

Table 1 presents the peak heating and cooling demands for each building, along with their annual heating and cooling energy requirements. The hospital exhibits significantly higher peak heating and cooling demands compared to all other users. Additionally, some users exchange heat and cooling for almost the entire year, while others, such as offices and schools, experience downtime periods (e.g., weekends or summer breaks for schools). Fig. 8 illustrates the hourly heating and cooling demand for the entire cluster of buildings. A peak heating demand of 2777.38 kW and a peak cooling demand of 3200.79 kW are observed. Fig. 8 further highlights the predominance of cooling needs in the selected locality.

3.2. Investigated scenarios

For the assumed case study, the following scenarios were simulated and compared:

- *Scenario No. 0* (or Base Case). The heating and cooling demands of each building are covered by using systems installed onsite without being connected to a DHN. More specifically, NG boilers and air-cooled chillers are reference technologies in winter in summer, respectively. The NG consumption of the boilers is calculated considering a constant energy efficiency of 0.95. Regarding air-cooled chillers, data provided in datasheets [46] allowed to relate EER values to the evaporator outlet fluid temperature and the

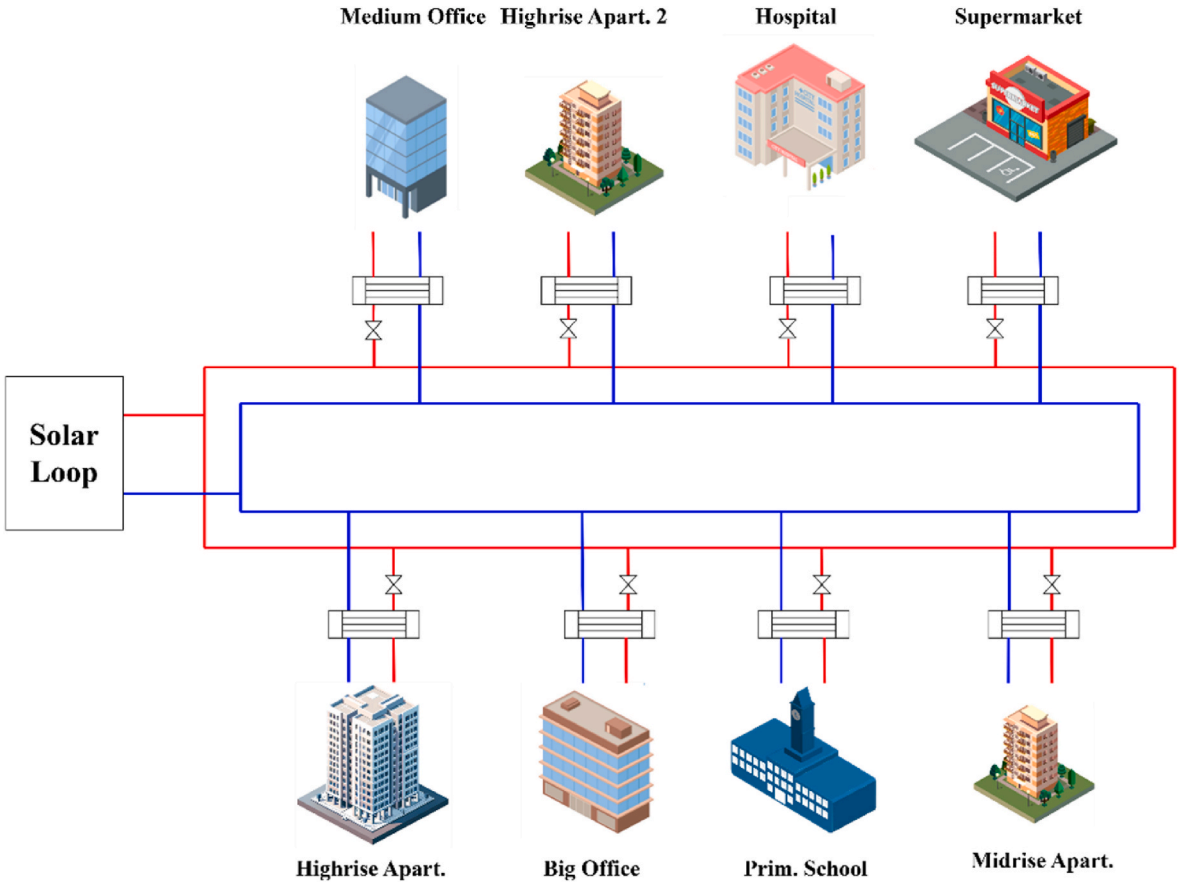

Fig. 5. Representation of buildings cluster of the case study.

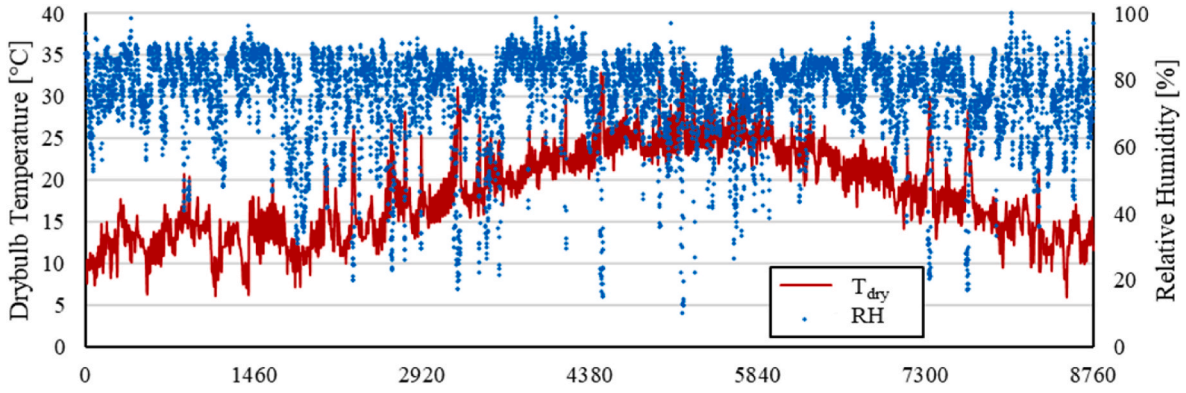

Fig. 6. Yearly profiles of ambient temperature and relative humidity in Palermo.

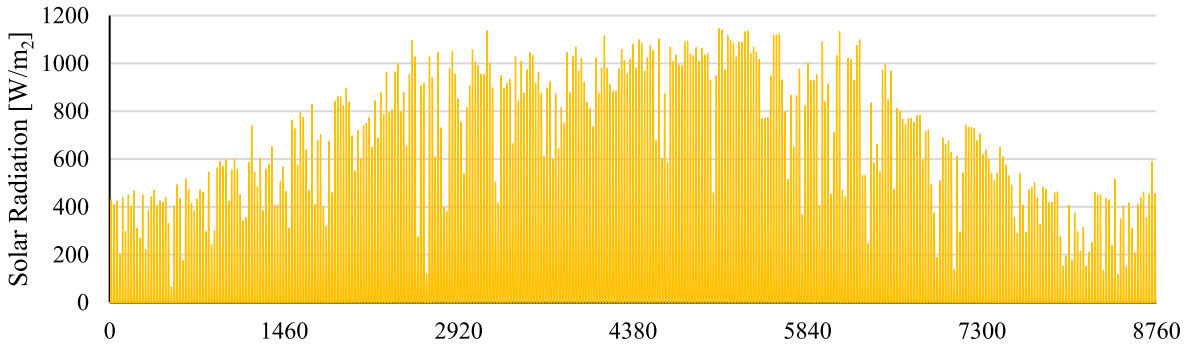

Fig. 7. Yearly profile of global solar radiation on a horizontal plane in Palermo.

Table 1
Yearly energy demand and peak in the demand of each user of the cluster.

User	Heating Peak	Cooling Peak	Heating Energy	Cooling Energy
	[kW]	[kW]	[MWh]	[MWh]
Medium Office	194.93	191.15	54.63	91.21
Highrise Apart. 2	366.86	493.91	280.23	628.86
Hospital	513.67	1114.72	935.12	907.65
Supermarket	301.59	235.88	240.14	117.92
Midrise Apart.	482.78	408.10	627.79	447.99
Prim. School	640.84	267.81	157.97	177.62
Big Office	474.76	656.24	320.28	196.01
HighRise Apart.	479.56	657.44	394.80	884.90

ambient temperature. This scenario is a baseline to compare the potential benefits arising through the integration of DHNs.

- *Scenario No. 1.* A DHN powered by a solar collector field and seasonal storage is assumed to cover the heating and cooling demands of the cluster. During winter, water at 60 °C circulates in the supply ring of the DHN, thus being eligible as a "low-temperature DHN". During the summer, to meet cooling demand, ABSs at the user are installed within each substation. Then, to ensure efficient operation of these devices, the temperature of the supply ring is increased up to 85 °C. Thanks to the operating temperature, it is not necessary for a temperature boost at the user substation to make the use of a plate exchanger feasible. Since the solar collector field cannot provide an adequate supply temperature at all times of the year, an auxiliary NG boiler was included in the solar loop.

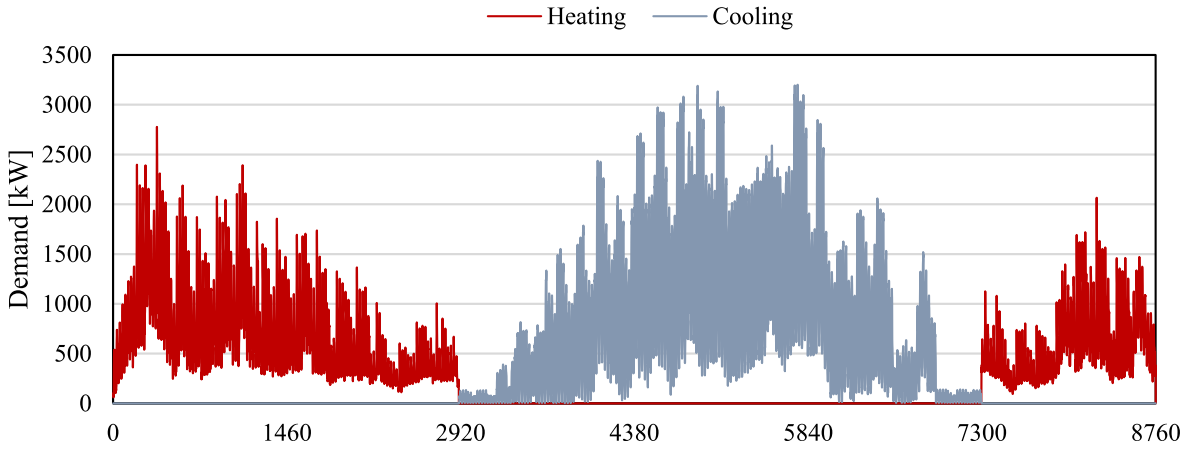

Fig. 8. Yearly profile of heating and cooling demands of the cluster.

- *Scenario No. 2.* An ultra-low temperature network is assumed, supplied by a solar field coupled with TES. The network operates at 20 °C during the winter. For this reason, booster HPs are required within the user substations to raise the water temperature to the level needed by the local SH systems. In the summer, conversely, chilled water at 7 °C is produced by a centralized ABS (located in the solar field) powered by heat from the solar plant or by the auxiliary air-cooled chiller.

It must be noted that both Scenario No. 1 and Scenario No. 2 do not comply perfectly with the definition of 4G- and 5GDHN [2,6,25]. For this reason, it was decided to define the network as a "low temperature", in the Case of Scenario No. 1, and "ultra-low temperature" in the case of Scenario No. 2. Indeed, focusing on Scenario No. 1, in the heating period, the network could be assumed to be as 4GDHN since hot water at 60 °C is provided as suggested in [6]. However, in summer, the operating temperature is higher than the 60 °C to ensure the correct operation of ABSs. For Scenario No. 2, the system can be classified as a 5GDHN only during winter when the network is maintained at 20 °C [2]. In summer, conversely, chilled water is supplied directly to users, becoming a district cooling network.

Finally, it is important to note that in Scenario No. 2, chilled water is not produced by the W/W HPs installed in each substation. This approach maximizes the utilization of thermal energy from the solar field, which is abundantly available during summer. As a result, the benefits are twofold: (i) a significant reduction in electricity consumption during the summer is achieved with a consequent decrease in PE, and (ii) an increase in the operating hours of both the network and the solar plant is realized, leading to a more efficient distribution of capital costs throughout the year.

3.3. Data and main assumptions

To appropriately size the solar field, guidelines for centralized SDH suggest, as per [44], that 1.4–2.4 m^2 of flat-plate collector surface per MWh of annual heat demand is optimal for central solar heating plants with seasonal storage. The annual heat demand was determined by aggregating the thermal energy requirements, including the energy needed by the ABSs. Based on the performance curve of the selected chiller [45], a conservative COP of 0.51 was assumed, resulting in a total yearly thermal energy demand of 9780 MWh. Using these calculations, a solar collector field with a surface area of 12,000 m^2 was deemed sufficient, considering the use of evacuated tube collectors. Furthermore, the guidelines presented by Schmit et al. [44] specify that the thermal storage should have a volume of 1.4–2.1 m^3 per m^2 of flat-plate collector surface. Therefore, given the thermal demand of the users and the selected collector surface area, a PTES of 30,000 m^3 was found to be suitable for the case study. To ensure realistic heat loss behavior from the storage, insulation with a 1-m thickness of Extruded Polystyrene was chosen, in alignment with [42]. The proposed design of PTES volume and collectors' surface was also chosen to ensure it was compliant with the fifteen SDH plants presented in a review on large-scale PTES [41].

The DHN was designed by relying on steady-state simulations conducted in the Energy Equation Solver [55], following the same procedures presented in a previous paper by the authors [35]. The analysis prioritized the cooling demand due to its predominance for the selected site. A conservative approach was adopted to select the diameter by assuming the scenario where all users simultaneously demand their peak load. Given the network's composition of 8 users, a simultaneity factor of 0.95 was applied to account for concurrent usage. In the context of the 4GDHN, where each user is equipped with an ABS operating with supply and evaporator temperatures set at 85 °C and 7 °C respectively, the COP of the ABS was estimated, based on the performance curve outlined in Ref. [45], and then the heat needed by each user to feed the chiller was calculated. In Scenario No. 1, the network operates with an average temperature difference of 20 °C between the supply and return loops, leading to a lower flow rate in the loops. In Scenario No. 2, the average temperature difference between the loops is 5 °C in winter and summer resulting in higher flow rates, and larger network diameter. With a uniform distance of 200 m between users and consistent branch diameters, the findings indicated that DN 200 pipes were necessary to maintain a specific pressure drop between 150 Pa/m and 250 Pa/m [56] for Scenario No.1, whereas DN 300 pipes were required for Scenario No.2. The selected pipe diameters for the two scenarios, DN 200 in Scenario No. 1 and DN 300 in Scenario No. 2, resulted in specific pressure drops of 249 Pa/m and 143.5 Pa/m, respectively, in the most stressed branch. Adjusting the diameter to DN 250 for both scenarios would result in pressure drops outside the threshold values recommended in [56], specifically 83 Pa/m for Scenario No. 1 and 352 Pa/m for Scenario No. 2.

In the substation presented in this work for Scenario No.2 (compatible with 5GDHN operation), the flow from the network can interact with an exchanger or with a reversible HP, based on supply water temperature. However, no scenarios involve the prosumers in this work, as the main aim is to investigate the potential benefits of solar-driven DHC technologies in a Mediterranean climate. Investigation of prosumers, as discussed in Refs. [57,58] requires a standalone depth analysis of their interactions with the network, influenced by both topology and location, that will surely be evaluated in future works.

A sensitivity analysis should be conducted to determine the optimal size of each energy source involved. This would allow for the proper sizing of all components, including solar panels, PTES, absorption chillers, and auxiliary chillers. However, in this stage, the component sizes were assumed based on rules of thumb or results available from other studies. Specifically:

- The size of HPs was selected based on meeting thermal demand while avoiding oversizing, following the same approach used for absorption chillers in user substations.
- The central absorption chiller in Scenario 2 was designed to operate near maximum system capacity, rather than the total capacity of all users.
- Two air-cooled chillers of 1.4 MW each were included to support the absorption chiller.
- The boiler capacity was set at 1.4 MW to adequately support the solar collectors in Scenario 1.

To provide a comprehensive overview, the sizes and details of the assumed machines are presented in Table 2. The selected components incorporate some of the most novel and efficient technologies available, including chillers and HPs with inverter compressors, which provide higher energy savings compared to conventional on-off devices [59]. Moreover, the assumed ABSs can also produce chilled water, even when powered by low-temperature heat, although with reduced capacity.

Table 2
Technical Details of Absorption chiller, W/W HPs, and air-cooled chiller.

	Absorption Chiller [60]	W/W Reversible HP [61]	Air Cooled Chiller [62]
Mixture/ Refrigerant	Water-Lithium Bromide	R1234ze/R515B	R513A
Compressor Type	–	Screw (Inverter)	Screw (Inverter)
No. Refrigerant Circuits	–	2–3	1–2
No. Of Compressors	–	2–3	1–2
Heating Capacity	–	243–1212 kW	–
Cooling Capacity	179–1125 kW (users) 3024 kW (main)	217–1097 kW	294–1089 kW (users) 1423 kW (main)
Chilled Water Temperature	1–10 °C	−8 to 7 °C	−1 to 18 °C
Hot Water Temperature	70–160 °C	45–65 °C	–

To model HPs, ABSs and air-cooled chillers, the curves in Fig. 9 were selected as they represent complete and publicly available data according to the knowledge of the authors. The curves were determined to be most suitable for use in the intended dynamic model owing to their recency, compliance with the components assumed in this study, and the level of detail provided.

3.4. Energy and environmental performance indicators

To quantify the energy and environmental benefits, two indicators were considered. Since two energy vectors were involved (i.e., electricity to drive chillers, HPs, and district network pumps, and NG consumption for boilers), they were converted into PE consumption, PE_y, as shown in Eq. (6):

$$PE_y = \sum_{i=1}^{8760} \left(f_{PE,ng} \cdot Q_{NG,i} + f_{PE,e} \cdot E_{e,i} \right) \quad (6)$$

where $Q_{NG,i}$ represents the NG thermal energy consumption during i-th hour, and $E_{e,i}$ is the total electricity consumption, including pumps, chillers, or HPs. $f_{PE,ng}$ and $f_{PE,e}$ are the PE conversion factors for NG and grid electricity, respectively equal to 1.05 and 2.42 as provided in Ref. [63].

To quantify the environmental benefits, the annual CO_2 emissions were estimated by using an approach similar to Eq. (6), using a conversion factor for stationary combustion of NG of 181 g_{CO2}/kWh, as reported in Ref. [64], and a conversion factor for electric energy consumption of 225 g_{CO2}/kWh corresponding to the Italian energy mix in 2023 as suggested in [65].

4. Results and discussions

In this section, the results of the dynamic simulation are presented and discussed. First, the energy consumption and emissions of the base case (Scenario No. 0) are shown. Then, a detailed analysis of the thermohydraulic operation of the DHN in Scenarios No. 1 and No. 2 is provided, with insights into the annual energy consumption and CO_2 emissions.

4.1. Results for "Scenario No. 0"

As previously mentioned, in this scenario, each user meets its heating and cooling demands using onsite boilers and air-cooled chillers without being connected to a DHN. In Table 3, yearly PE consumption and CO_2 emissions for the cluster are shown. Despite the cooling demand being more prevalent than heating and the different PE conversion factors, the PE used for cooling is lower than the one used for heating. This difference is consequent to the better performance of air-cooled chillers compared to boilers, which leads to lower PE consumption. Zooming on users, the hospital is the largest energy consumer, with 1446 MWh $\cdot y^{-1}$, followed by the mid-rise apartments at 896 MWh $\cdot y^{-1}$, accounting for 29.6% and 18.3% of the total consumption, respectively.

Table 3
PE consumption and CO_2 emissions for Scenario No. 0.

		Boilers	Air-Cooled Chillers	Total
PE	[MWh $\cdot y^{-1}$]	3327.9	1549.6	4877.6
CO_2 Emissions	[t$\cdot y^{-1}$]	573.7	178.8	752.8

4.2. Analysis of the network operation for Scenarios No. 1 and no. 2

Hourly simulations in TRNSYS, enabled monitoring of the supply water temperature T_s, the storage temperature T_{sto} (Fig. 10), and the operation of auxiliary systems throughout the year (Fig. 11).

Fig. 10 indicates that in Scenario No. 1, the average temperature of the storage during the first months is lower than the setpoint required by the supply network (i.e., 60 °C). Then, to meet the required temperature setpoint, the auxiliary boiler in the solar loop is activated from 370 to 1981 h, as also shown by the blue line in Fig. 11. In this respect, a peak of 598 kW in boiler daily consumption is found. Conversely, in Scenario No. 2, due to the lower setpoint temperature (i.e., 20 °C), the PTES is sufficient to meet the entire thermal energy demanded by the booster HPs installed within each substation.

In summer, in Scenario No. 1, the boiler activates at the beginning of the summer and after 5513 h to support the solar field, when the average PTES temperature falls below 85 °C, which is the temperature required by ABSs installed within users' substations. Conversely, in Scenario No. 2, the PTES temperature drops below 85 °C (Fig. 10) after 4403 h, necessitating the auxiliary air-cooled chiller to alternate between activation and deactivation to support the ABS (Fig. 11). In Scenario No. 1, the auxiliary boiler remains active for a shorter period, with a peak daily average thermal power of 814 kW.

Finally, as shown in Fig. 11, the power required for pumping is significantly lower than other components for both scenarios in such a small network.

In Fig. 12, the amount of heat loss (positive in winter and negative in summer) in Scenarios No. 1 and No. 2 are shown. A comparison of the profiles highlights the potential advantages of an ultra-low temperature network (Scenario No. 2) over low-temperature networks (Scenario No. 1). Indeed, in Scenario No. 2 losses do not exceed 11 kW during the heating period or fall below −15 kW during the cooling period. In contrast, Scenario No. 1 exhibits a peak of 36.8 kW during the cooling period and 27.1 kW during the heating period.

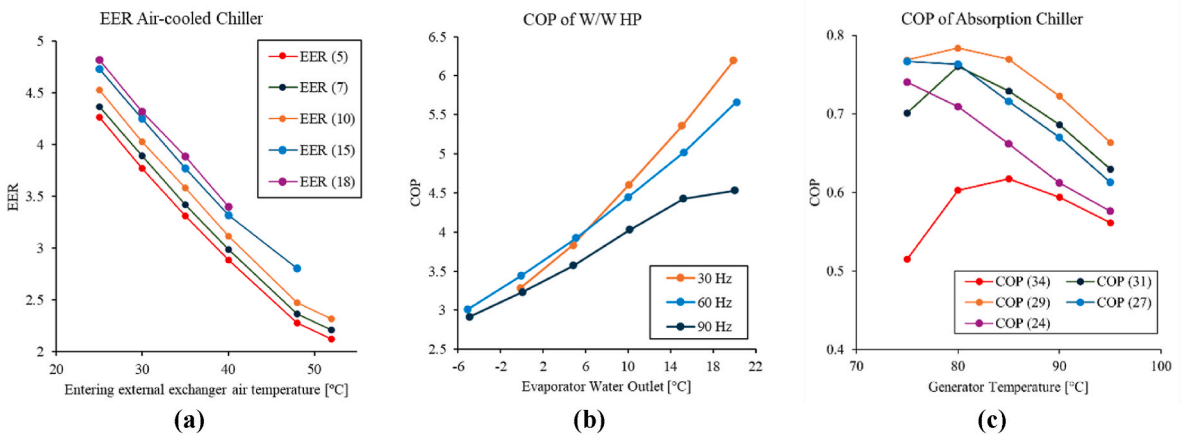

Fig. 9. Performance curves of (a) air-cooled chiller [46], (b) W/W HP [48], and (c) absorption chiller [45] implemented in TRNSYS model.

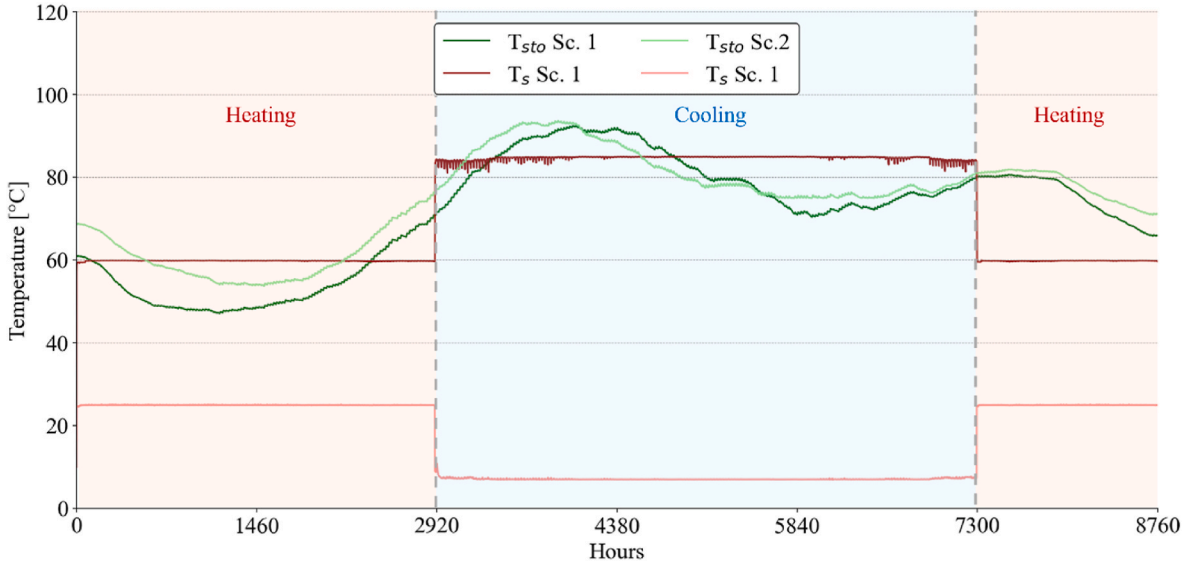

Fig. 10. Hourly temperature profile in the DHN and storage.

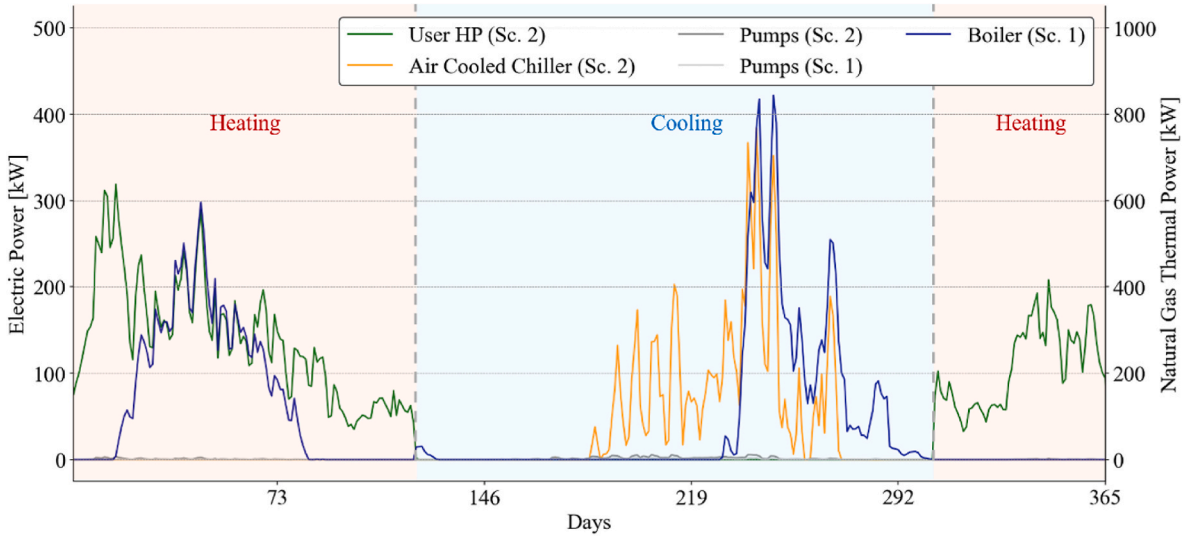

Fig. 11. Daily average power behavior of different systems in the two scenarios.

Over the entire year, the total heat losses (which includes the ones from the DHN and the PTES) amount to 723.3 MWh $\cdot y^{-1}$ in Scenario No. 1. Conversely, Scenario No. 2 exhibits significantly lower losses at 317.8 MWh ·y-1, which corresponds to 60.8% of the losses in Scenario No. 1. When considering only pipe-related heat losses, Scenario 2 accounts for just 32.6% of those in Scenario 1.

Although heat losses in the PTES are comparable between the two scenarios, the heat losses in the supply loop are notably lower in Scenario No. 2. The temperature within the PTES is similar in both scenarios, thus leading to comparable PTES heat losses: 310.9 MWh $\cdot y^{-1}$ in Scenario No. 1 and 305.4 MWh $\cdot y^{-1}$ in Scenario No. 2.

4.2.1. *Pressure profiles*

Fig. 13 illustrates the pressure profiles in Scenario No. 1. P_{0s} and P_{0r} represent the head pressure for the supply and return side, respectively, while P_{0s*} and P_{0r*} indicate the intake pressure of the pumps for the supply and return side. Looking at Fig. 13, during the winter, in Scenario No. 1, the pressure drops are lower than in the summer, because the network was designed based on the peak of the cooling demand. Moreover, in summer, when the COP_{ABS} is very low, the demand for higher flow rates results in increased pressure drops. The electric power used by the pumps, respectively $P_{pump,s}$ and $P_{pump,r}$ for supply and return side, is greater in summer with a peak of about 5 kW.

In Fig. 14, pressure profiles in the supply and return ring in Scenario No. 2 are illustrated. In this scenario, pressure drops are similar in the heating and cooling periods. This is due to the slightly higher cooling energy demand, including peak load, compared to the heating load in this case study, as previously presented in Table 1. Additionally, in this scenario, the water flow rate is comparable in the heating and cooling periods, differently from Scenario No. 1, where the heat demand depends on the COP_{ABS}, resulting in higher flow rates during the cooling period. Consequently, the pumping power in Scenario No. 2 is consistently around 5–10 kW for both the supply and return sides throughout the year, compared to peaks of 5 kW observed in Scenario No. 1. This happens as, despite the pressure drops of Scenario No. 1 are slightly higher in summer, the flowrates in Scenario No. 2 are about 4 times higher than in Scenario No. 1.

Focusing on a representative winter and summer week, starting on December 10th and July 23rd, respectively, as shown in Fig. 15, the key differences between the two scenarios become evident. In winter, the

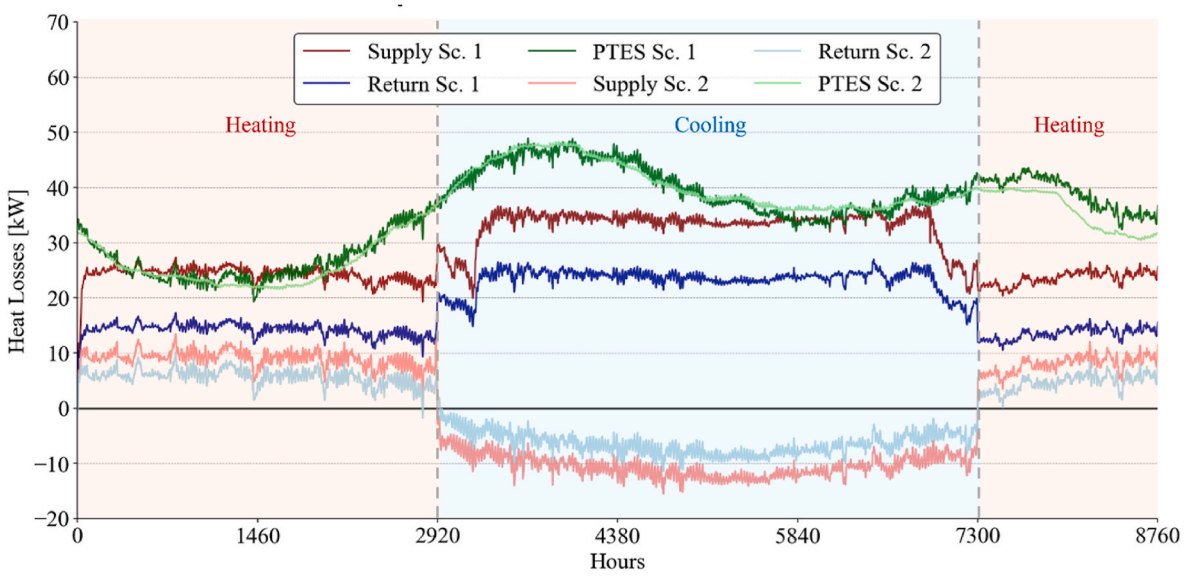

Fig. 12. Overall heat losses in the DHN in Scenarios No. 1 and No. 2.

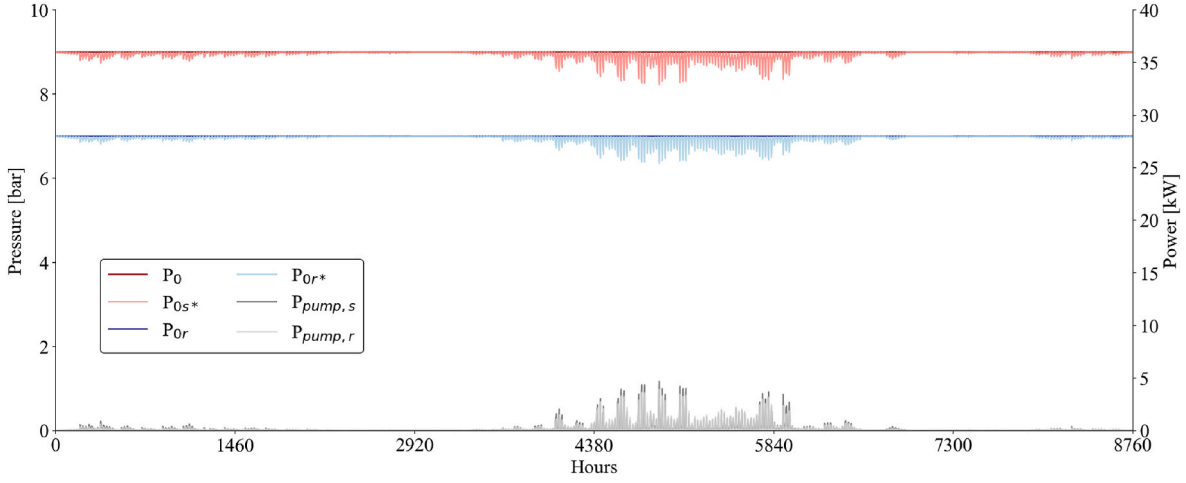

Fig. 13. Pressure profile and electric power demand of pumps in Scenario No. 1.

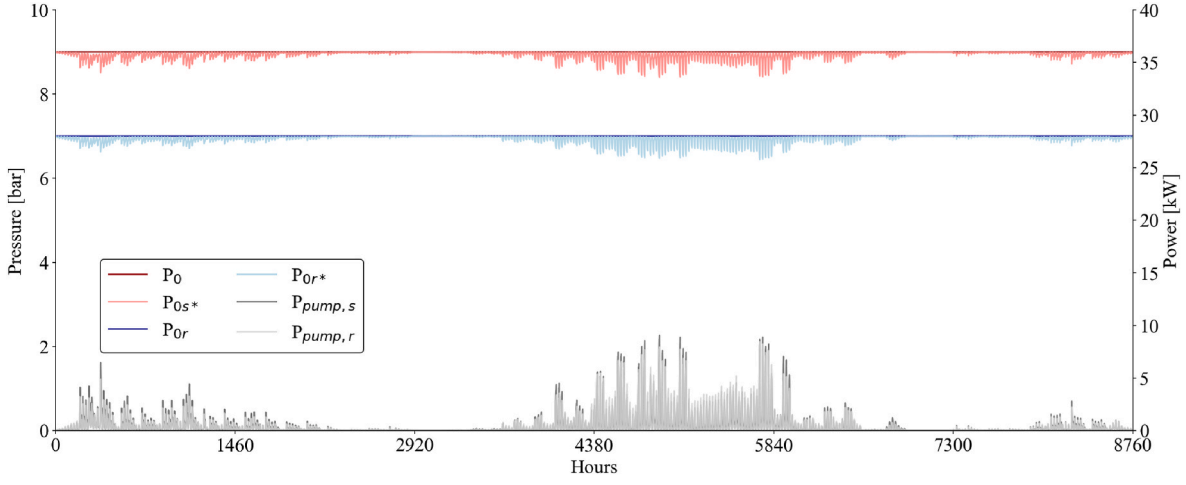

Fig. 14. Pressure profile and electric power demand of pumps in Scenario No. 2.

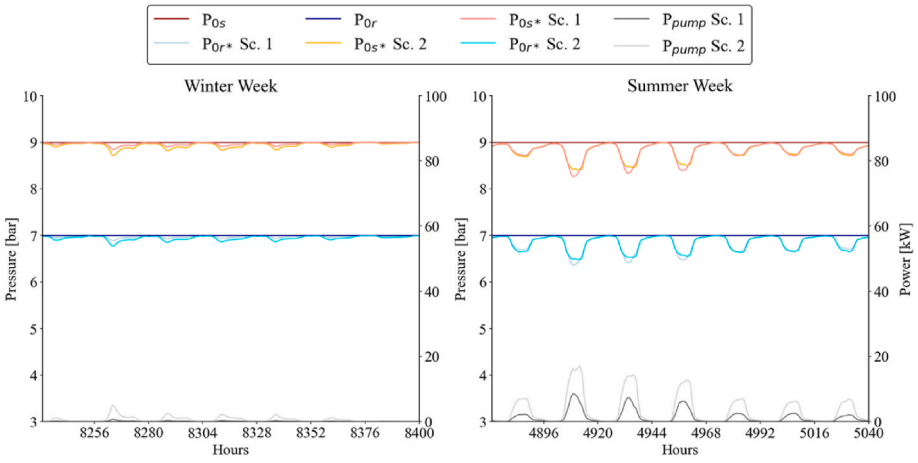

Fig. 15. Pressure profile in two typical weeks in winter and summer.

pressure drops are higher in Scenario No. 2, averaging 1.9 to 2.1 times those in Scenario No. 1 for the supply and return sides, respectively. In summer, the opposite occurs, with pressure drops on the supply side of Scenario No. 1 reaching up to 1.2 times those in Scenario No. 2, and the same on the return side. However, the pumping power does not reflect these trends. In winter, the pumping power is almost negligible for Scenario No. 1. In the summer, on the second day, the peak power in Scenario No. 1 is 0.5 times the power of Scenario No. 2. Furthermore, even for the most stressed user (located at the furthest point in the network), a differential pressure greater than 1 bar between the supply and return sides is maintained, confirming the network's proper design in compliance with the previously cited guidelines [56].

4.3. Yearly results for Scenarios No. 1 and no. 2

Table 4 summarizes the energy and environmental results for Scenarios No. 1 and 2. As it can be noted, in both scenarios, there is a significant reduction in overall PE consumption and CO_2 emissions. In Scenario No. 1, the solar field, capable of producing over 7 MWh·y^{-1} of thermal energy, reduces PE consumption and emissions by 82% and 80%, respectively. In this scenario, the boiler is used mainly during the heating season, as the lower solar radiation was insufficient to consistently produce water at 60 °C (temperature required by the supply ring of the DHN). During the cooling season, the heat stored in the PTES during low-demand periods, limited PE needs to just 72.5 % of the PE consumption observed in Scenario No. 0. Up to 350 MWh·y^{-1} of thermal energy remains stored in the PTES, considering 75 °C as the lower boundary. Nevertheless, operating at a lower supply temperature will reduce user absorption chillers' cooling capacity by 20%, resulting in excessive oversizing of the machines.

In Scenario No. 2, although PE was required during the heating season to drive booster HPs, the reductions in PE consumption and CO_2 emissions were still significant (62% and 76.8%, respectively). Notably, while Scenario No. 1 shows comparable percentage reductions in emissions and PE consumption, the exclusive use of electricity as the energy input for Scenario No. 2 led to an emissions reduction 1.2 times greater than the PE reduction. This difference arises because the lower carbon intensity of electricity, compared to NG, leads to higher emissions savings per unit of PE consumed. As a result, even though the percentage reduction in PE consumption for Scenario No. 2 is lower, a total emissions reduction of 76.8% was achieved.

In Table 5, values of PE consumed by each component are shown. A comparison provides a clearer understanding of the benefits and limitations of each scenario. For instance, in Scenario No. 2, auxiliary systems did not consume PE during the heating season since, thanks to lower supply temperatures, the solar collectors were sufficient (i.e. 20 °C). However, since booster HPs are required within users' substation, the PE consumed by the user during the heating period (i.e., 1355.1 MWh·y^{-1}) is 3 times higher than the one consumed by the boiler in Scenario No. 1 (i.e., 449.6 MWh·y^{-1}). However, when electricity for booster HPs is produced in the case of high PV penetration, this configuration becomes very promising.

Lastly, regarding PE consumed for pumping, despite the lower pressure due to the larger pipe diameters in Scenario No. 2, PE consumption for pumping is 3.3 times higher than the one found in Scenario No. 1. This difference is evident in heating, where pumping energy in Scenario No. 2 is 7.7 times greater than the one found for Scenario No. 1. As previously mentioned (see Fig. 15), this is due to the higher water flow rate in Scenario no. 2.

5. Conclusions

In this work, a comparative energy of solar-powered DHCN serving a cluster of buildings in the Mediterranean climate was performed. A novel model compatible with fourth and fifth-generation DHCN was developed, powered by a solar collector system, an ABS, auxiliary systems, and seasonal TES. A cluster of eight users in Palermo (Southern Italy) was assumed as the case study. The design of network components and the thermal plant was tailored to meet the requirements of the connected building cluster, including the sizing of pipes, solar collectors,

Table 4
Energy and CO_2 emissions results of the Case Study Scenarios.

Scenarios	PE [MWh·y^{-1}]			CO_2 Emissions [tCO$_2$·y^{-1}]		
	Heating	Cooling	Total	Heating	Cooling	Total
No. 0	3327.9	1549.6	4877.5	574.0	178.8	752.8
No. 1	450.3	426.0	876.3 (−82%)	77.6	73.0	150.6 (−80%)
No. 2	1360.7	516.5	1877.2 (−62%)	126.5	48.0	174.5 (−76.8%)

Table 5
PE Consumption for each system used in the DHNs scenarios.

PE [MWh·y^{-1}]			
		Scenario No. 1	Scenario No. 2
Auxiliary System	Heating	449.6	0
	Cooling	420.7	502.2
Pumping	Heating	0.7	5.6
	Cooling	5.4	14.3
User HPs	Heating	0	1355.1

and TES. The model, developed using TRNSYS software, was tested across operational scenarios involving different methods of delivering heating and cooling energy to users of the cluster. Scenario No. 0, serving as the baseline, assumes that users autonomously meet their demands using gas boilers and air-cooled chillers. In Scenario No. 1, a network resembling a low-temperature operation is powered by solar collectors and a gas boiler. The DHN directly supplies users with 60 °C water during the heating period and 85 °C water during the cooling period to feed users' ABSs. In Scenario No. 2, an industrial ABS powered by hot water from the solar field is supported by an auxiliary chiller. On the network side, warm water at 20 °C is supplied during the heating period, with users equipped with W/W inverter HPs, while chilled water at 7 °C is provided during the cooling period. The results showed that both scenarios significantly reduced emissions, with savings of 80% in Scenario No. 1 and 76.8% in Scenario No. 2. PE consumption decreased from 4877.5 MWh in the baseline to 876.3 MWh in Scenario No. 1 and 1877.2 MWh in Scenario No. 2. Although larger pipe diameters were used in Scenario No. 2, the limited temperature difference between the supply and return sides resulted in pumping energy requirements that were 3.3 times higher than in Scenario No. 1. Due to the lower operating temperatures, heat losses in the pipes in Scenario No. 2 were only 32.6% of those in Scenario No. 1. However, this reduction in heat losses was insufficient to offset the increase in PE consumption associated with the use of user HPs in Scenario No. 2. These results demonstrated how the use of a last-generation network powered by RES brings considerable advantages in terms of resource savings and a significant reduction in CO_2 emissions, contributing to the transition towards the decarbonization of the urban sector. Economic analysis should be performed in the future to effectively propose sustainable solutions accelerating decarbonization in line with Europe's goals for 2050. To this end, a new analysis needs to be conducted with the aim of optimizing all the component sizes used in this study. It should consist of detailed cost analyses, considering PTES construction and auxiliary components, determining large-scale system feasibility and investment requirements.

Nomenclature

COP_{ABS}	Coefficient of performance of the absorption chiller
COP_{HP}	Coefficient of performance of the heat pump
c_w	Specific heat of water
$E_{e,i}$	Total electricity consumption during hour i
$f_{PE,e}$	Primary energy conversion factor for electricity
$f_{PE,ng}$	Primary energy conversion factor for natural gas
$\dot{m}_{ch}$	Flow rate of chilled water
$\dot{m}_{gen}$	Flow rate of the fluid feeding the absorption chiller generator
P_{0r}	Head pressure for the return side
P_{0r^*}	Intake pressure for the return side
P_{0s}	Head pressure for the supply side
P_{0s^*}	Intake pressure for the supply side
$P_{pump,s}$	Electric power used by the pump on the supply side
$P_{pump,r}$	Electric power used by the pump on the return side
PE_y	Yearly primary energy consumption
$\dot{Q}_{ch,max}$	Maximum amount of heat removable from chilled water
$\dot{Q}_{gen}$	The maximum theoretical amount of heat extractable from the fluid feeding the absorption chiller generator
$Q_{NG,i}$	Natural gas energy consumption in hour i
$\dot{Q}_{rated}$	Rated capacity of the absorption chiller
$\dot{Q}_{set}$	Heat removed from chilled water to reach setpoint
$T_{ch,in}$	Inlet temperature of the chilled water
$T_{ch,set}$	Setpoint temperature of chilled water
T_{dry}	Drybulb temperature
$T_{gen,in}$	Temperature of the hot fluid feeding the absorption chiller generator
$T_{gen,set}$	Minimum temperature of the hot fluid compatible with chiller operation
T_s	Water supply Temperature
T_{sto}	Average temperature in the storage

Acronyms

4GDHN	Fourth Generation District Heating Network
5GDHN	Fifth Generation District Heating Network
ABS	Absorption Chiller
CO_2	Carbon Dioxide
COP	Coefficient of Performance
DHC	District Heating and Cooling
DHCN	District Heating and Cooling Networks
DHN	District Heating Network
DHW	Domestic Hot Water
DN	Nominal Diameter
EER	Energy Efficiency Ratio
gCO_2	Grams Of Carbon Dioxide
HP	Vapor Compression Heat Pumps
IEA	International Energy Agency
NG	Natural Gas
PE	Primary Energy
PTES	Pit Thermal Energy Storage
PV	Photovoltaic
PVT	Photovoltaic Thermal
RES	Renewable Energy Source
RH	Relative Humidity
SC	Solar Cooling
SDH	Solar District Heating
SH	Space Heating
TES	Thermal Energy Storage
tCO_2	Tons Of Carbon Dioxide
TRNSYS	Transient System Simulation Tool
W/W	Water to Water

CRediT authorship contribution statement

Tancredi Testasecca: Writing – review & editing, Writing – original draft, Visualization, Software, Methodology, Investigation, Conceptualization. **Pietro Catrini:** Writing – review & editing, Writing – original draft, Methodology, Investigation, Data curation, Conceptualization. **Maurizio La Villetta:** Resources, Methodology, Investigation, Data curation. **Marco Beccali:** Writing – review & editing, Supervision, Resources, Methodology, Investigation. **Antonio Piacentino:** Writing – review & editing, Supervision, Resources, Methodology, Investigation, Conceptualization.

Declaration of competing interest

The authors declare that they have no known competing financial interests or personal relationships that could have appeared to influence the work reported in this paper.

Acknowledgments

The authors acknowledge the organizers of the 19th Conference on Sustainable Development of Energy, Water and Environment Systems (SDEWES), held in Rome from 8 to September 12, 2024, for providing a valuable platform for knowledge exchange and discussion on sustainable energy systems. The conference facilitated the dissemination of this research and offered an important opportunity to engage with the international scientific community.

References

[1] IEA, Heating (2020). https://www.iea.org/reports/heating.
[2] H. Lund, P.A. Østergaard, T.B. Nielsen, S. Werner, J.E. Thorsen, O. Gudmundsson, et al., Perspectives on fourth and fifth generation district heating, Energy 227 (2021) 120520, https://doi.org/10.1016/j.energy.2021.120520.
[3] H. Lund, Renewable energy strategies for sustainable development, Energy 32 (2007) 912–919, https://doi.org/10.1016/j.energy.2006.10.017.
[4] R. Weiss, Decarbonised district heat, electricity and synthetic renewable gas in wind-and solar-based district energy systems, J. Sustain. Dev Energy, Water Environ. Syste. 9 (2021), https://doi.org/10.13044/j.sdewes.d8.0340.
[5] International Energy Agency (IEA), District Heating, 2023.
[6] H. Lund, S. Werner, R. Wiltshire, S. Svendsen, J.E. Thorsen, F. Hvelplund, et al., 4th generation district heating (4GDH). Integrating smart thermal grids into future sustainable energy systems, Energy 68 (2014) 1–11, https://doi.org/10.1016/j.energy.2014.02.089.

[7] G. Martinazzoli, D. Pasinelli, A.M. Lezzi, M. Pilotelli, Design of a 5th generation district heating substation prototype for a real case study, Sustainability 15 (2023) 2972, https://doi.org/10.3390/su15042972.

[8] M. Pellegrini, A. Bianchini, The innovative concept of cold district heating networks: a literature review, Energies 11 (2018), https://doi.org/10.3390/en11010236.

[9] Joint Research Centre and Institute for Environment and Sustainability, K. Mutka, P. Papillon, R. Kalf, G. Stryi-Hipp, W. Weiss, B. Sanner, A. Land, Common Vision for the Renewable Heating and Cooling Sector in Europe: European Technology Platform on Renewable Heating and Cooling, Publications Office of the European Union, Luxembourg, 2020–2030–2050, p. 2011, n.d.

[10] H. Averfalk, P. Ingvarsson, U. Persson, M. Gong, S. Werner, Large heat pumps in Swedish district heating systems, Renew. Sustain. Energy Rev. 79 (2017) 1275–1284, https://doi.org/10.1016/j.rser.2017.05.135.

[11] D. Tschopp, Z. Tian, M. Berberich, J. Fan, B. Perers, S. Furbo, Large-scale solar thermal systems in leading countries: a review and comparative study of Denmark, China, Germany and Austria, Appl. Energy 270 (2020), https://doi.org/10.1016/j.apenergy.2020.114997.

[12] H. Lund, P.A. Østergaard, D. Connolly, I. Ridjan, B.V. Mathiesen, F. Hvelplund, et al., Energy storage and smart energy systems, Intern. J. Sustain. Energy Planning Manag. 11 (2016) 3–14, https://doi.org/10.5278/ijsepm.2016.11.2.

[13] Andersen J. Dannemand, L. Bødker, M.V. Jensen, Large thermal energy storage at marstal district heating. Proceedings of the 18th International Conference on Soil Mechanics and Geotechnical Engineering, Paris, 2013.

[14] W. Weiss, M. Spörk-Dür, Global Market Development and Trends 2021 Detailed Market Figures 2020 SOLAR HEAT WORLD WIDE, 2022, https://doi.org/10.18777/ieashc-shw-2022-0001 n.d.

[15] J. Deng, R.Z. Wang, G.Y. Han, A review of thermally activated cooling technologies for combined cooling, heating and power systems, Prog. Energy Combust. Sci. 37 (2011) 172–203, https://doi.org/10.1016/j.pecs.2010.05.003.

[16] M. Bilardo, M. Ferrara, E. Fabrizio, Performance assessment and optimization of a solar cooling system to satisfy renewable energy ratio (RER) requirements in multi-family buildings, Renew. Energy 155 (2020) 990–1008, https://doi.org/10.1016/j.renene.2020.03.044.

[17] K. Salhi, M.M. Hadjiat, A. Bourabaa, Study of a Single Effect Absorption Refrigeration System Using Geothermal Sources in Algeria, 2015.

[18] F. Calise, L. Libertini, M. Vicidomini, Design and optimization of a novel solar cooling system for combined cycle power plants, J. Clean. Prod. 161 (2017) 1385–1403, https://doi.org/10.1016/j.jclepro.2017.06.157.

[19] D.O. Machado, W.D. Chicaiza, J.M. Escaño, A.J. Gallego, G.A. de Andrade, J. E. Normey-Rico, et al., Digital twin of an absorption chiller for solar cooling, Renew. Energy 208 (2023) 36–51, https://doi.org/10.1016/j.renene.2023.03.048.

[20] J. Freeman, C.N. Markides, A solar diffusion-absorption refrigeration system for off-grid cold-chain provision. Part I: model development and experimental calibration, Renew. Energy 230 (2024), https://doi.org/10.1016/j.renene.2024.120718.

[21] J. Freeman, C.N. Markides, A solar diffusion-absorption refrigeration system for off-grid cold-chain provision, part II: system simulation and assessment of performance, Renew. Energy 230 (2024), https://doi.org/10.1016/j.renene.2024.120717.

[22] J. Persson, M. Westermark, Low-energy buildings and seasonal thermal energy storages from a behavioral economics perspective, Appl. Energy 112 (2013) 975–980, https://doi.org/10.1016/j.apenergy.2013.03.047.

[23] W. Weiss, M. Spörk-Dür, Solar heat worldwide 2024. https://doi.org/10.18777/ieashc-shww-2024-0001, 2024.

[24] International Energy Agency Technology, SUSTAINABLE DISTRICT COOLING GUIDELINES, 2019.

[25] P. Sorknæs, P.A. Østergaard, J.Z. Thellufsen, H. Lund, S. Nielsen, S. Djørup, et al., The benefits of 4th generation district heating in a 100% renewable energy system, Energy 213 (2020), https://doi.org/10.1016/j.energy.2020.119030.

[26] J.S. Figueira, A. García Gil, A. Vieira, A.K. Michopoulos, D.P. Boon, F. Loveridge, et al., Shallow geothermal energy systems for district heating and cooling networks: review and technological progression through case studies, Renew. Energy 236 (2024), https://doi.org/10.1016/j.renene.2024.121436.

[27] F. Calise, F.L. Cappiello, L. Cimmino, M. Dentice d'Accadia, M. Vicidomini, A comparative thermoeconomic analysis of fourth generation and fifth generation district heating and cooling networks, Energy 284 (2023), https://doi.org/10.1016/j.energy.2023.128561.

[28] F. Calise, F.L. Cappiello, L. Cimmino, M. Vicidomini, F. Petrakopoulou, Thermoeconomic analysis of a novel topology of a 5th generation district energy network for a commercial user, Appl. Energy 371 (2024), https://doi.org/10.1016/j.apenergy.2024.123718.

[29] L. De Rosa, M. Martínez, J.I. Linares, C. Mateo, T. Gomez, R. Cossent, et al., Design and assessment of energy infrastructure in new decarbonized urban districts: a Spanish case study, Energy Rep. 11 (2024) 4631–4641, https://doi.org/10.1016/j.egyr.2024.04.037.

[30] A. Mugnini, G. Comodi, A. Arteconi, Heat pumps to upgrade existing CHP-DHN systems towards new generation thermal networks, Energy Rep. 12 (2024) 820–833, https://doi.org/10.1016/j.egyr.2024.06.063.

[31] Y. Xu, C. Zhan, A.R. Jensen, M. Gao, W. Kong, J. Fan, Thermo-economic analysis of a solar district heating plant with an air-to-water heat pump, Renew. Energy 237 (2024) 121490, https://doi.org/10.1016/j.renene.2024.121490.

[32] E. Ghirardi, G. Brumana, G. Franchini, Comparison between cold and hot network in a solar district cooling system, J. Phys. Conf. Ser. 2893 (2024), https://doi.org/10.1088/1742-6596/2893/1/012031. Institute of Physics.

[33] R. Ismaen, T.Y. Elmekkawy, S. Pokharel, A. Elomri, M. Al-Salem, Solar technology and district cooling system in a hot climate regions: optimal configuration and technology selection, Energies 15 (2022), https://doi.org/10.3390/en15072657.

[34] M. Sadi, A. Arabkoohsar, Exergy, economic and environmental analysis of a solar-assisted cold supply machine for district energy systems, Energy 206 (2020), https://doi.org/10.1016/j.energy.2020.118210.

[35] T. Testasecca, P. Catrini, M. Beccali, A. Piacentino, Dynamic simulation of a 4th generation district heating network with the presence of prosumers, Energy Convers. Manag. X (2023), https://doi.org/10.1016/j.ecmx.2023.100480.

[36] University of Wisconsin–Madison: Solar Energy Laboratory, TRNSYS 17, a Transient Simulation Program, 1975.

[37] G. Barone, A. Buonomano, C. Forzano, G.F. Giuzio, A. Palombo, Increasing renewable energy penetration and energy Independence of island communities: a novel dynamic simulation approach for energy, economic, and environmental analysis, and optimization, J. Clean. Prod. 311 (2021) 127558, https://doi.org/10.1016/j.jclepro.2021.127558.

[38] Z. Meng, Z. Huo, S. Dong, Y. Liu, S. Zhai, C. Ding, et al., Simulation study on the system performance of solar-ground source heat pump using return water of the district heating network as supplementary heating, Renew. Energy 231 (2024) 120906, https://doi.org/10.1016/j.renene.2024.120906.

[39] M. Bilardo, F. Sandrone, G. Zanzottera, E. Fabrizio, Modelling a fifth-generation bidirectional low temperature district heating and cooling (5GDHC) network for nearly zero energy district (nZED), Energy Rep. 7 (2021) 8390–8405, https://doi.org/10.1016/j.egyr.2021.04.054.

[40] A. Buscemi, M. Beccali, S. Guarino, V. Lo Brano, Coupling a road solar thermal collector and borehole thermal energy storage for building heating: first experimental and numerical results, Energy Convers. Manag. 291 (2023) 117279, https://doi.org/10.1016/j.enconman.2023.117279.

[41] Y. Xiang, Z. Xie, S. Furbo, D. Wang, M. Gao, J. Fan, A comprehensive review on pit thermal energy storage: technical elements, numerical approaches and recent applications, J. Energy Storage 55 (2022), https://doi.org/10.1016/j.est.2022.105716.

[42] E. Guelpa, V. Verda, Thermal energy storage in district heating and cooling systems: a review, Appl. Energy 252 (2019) 113474, https://doi.org/10.1016/j.apenergy.2019.113474.

[43] S.A. Klein, W.A. Beckman, J.W. Mitchell, J.A. Duffie, N.A. Duffie, T.L. Freeman, et al., TRNSYS 17 - Mathematical Reference, 2012.

[44] T. Schmidt, D. Mangold, H. Müller-Steinhagen, Central solar heating plants with seasonal storage in Germany, Sol. Energy 76 (2004) 165–174, https://doi.org/10.1016/j.solener.2003.07.025.

[45] MAYA - A YAZAKI CORPORATION JAPAN JOINT VENTURE COMPANY, REFRIGERATORI AD ASSORBIMENTO ALIMENTATI AD ACQUA CALDA SERIE WFC n.d. https://maya-airconditioning.com/wp-content/uploads/2022/10/WFC-Series-LD_001_IT-1.pdf. (Accessed 17 November 2024).

[46] Clivet SCREWLine3 [online]. Available: https://clivet.org/images/pdf/hava-khonak/Screw/WDAT-SL3/BT14D018GB-00_PRELIMINARY_01.pdf n.d.

[47] G. Ala, P. Catrini, M.G. Ippolito, M La Villetta, S. Licciardi, R. Musca, et al., A workflow for thermal and electrical Co-Simulation of energy systems. Asia Meeting on Environment and Electrical Engineering (EEE-AM), IEEE, 2023, pp. 1–6, https://doi.org/10.1109/EEE-AM58328.2023.10394689, 2023.

[48] F. Hüsing, Modelling of inverter heat pumps in TRNSYS. Proceedings of the ISES EuroSun 2020 Conference – 13th International Conference on Solar Energy for Buildings and Industry, International Solar Energy Society, Freiburg, Germany, 2020, pp. 1–8, https://doi.org/10.18086/eurosun.2020.04.08.

[49] Johnson Controls-Hitachi Air Conditioning, Centrifugal chiller high efficiency GFG-S/SIT series GXG-S/SIT series GSG-S/SIT series n.d. https://www.jci-hitachi.com/. (Accessed 8 August 2024).

[50] Y.A. Çengel, M.A. Boles, Thermodynamics: an Engineering Approach, McGraw-Hill Higher Education, 2006.

[51] EnergyPlus, Weather data by location n.d. https://energyplus.net/weather-location/europe_wmo_region_6/ITA/ITA_Palermo.164050_IWEC. (Accessed 5 October 2023).

[52] A. Piacentino, C. Barbaro, A comprehensive tool for efficient design and operation of polygeneration-based energy μgrids serving a cluster of buildings. Part II: analysis of the applicative potential, Appl. Energy 111 (2013) 1222–1238, https://doi.org/10.1016/j.apenergy.2012.11.079.

[53] Energy plus n.d.

[54] U.S. Department of Energy. Prototype building models n.d. https://www.energycodes.gov/prototype-building-models (accessed September 26, 2023).

[55] F.-C. Software, EES_manual, pdf, 2011, pp. 210–212.

[56] Gerhard Oppermann, Othmar Arnold, Joachim Ködel, Marcel Büchler, , et al. Martin Jutzeler, et al., Teleriscaldamento/Teleraffreddamento 2020, 2018.

[57] L. Brand, A. Calvén, J. Englund, H. Landersjö, P. Lauenburg, Smart district heating networks - a simulation study of prosumers' impact on technical parameters in distribution networks, Appl. Energy 129 (2014) 39–48, https://doi.org/10.1016/j.apenergy.2014.04.079.

[58] M. Gross, B. Karbasi, T. Reiners, L. Altieri, H.J. Wagner, V. Bertsch, Implementing prosumers into heating networks, Energy 230 (2021), https://doi.org/10.1016/j.energy.2021.120844.

[59] D.M. Kumar, P. Catrini, A. Piacentino, M. Cirrincione, Advanced modeling and energy-saving-oriented assessment of control strategies for air-cooled chillers in space cooling applications, Energy Convers. Manag. 291 (2023) 117258, https://doi.org/10.1016/j.enconman.2023.117258.

[60] YHAU-CL/CH low leaving chilled water supply two-stage single effect hot water absorption chiller mod B. YORK n.d. https://docs.johnsoncontrols.com/chillers/v/u/YORK/en-US/YHAU-CL/CH-Mod-B-Low-Leaving-Chiller-Water-Supply-Two-

Stage-Single-Effect-Hot-Water-Absorption-Chiller-Installation-Commissioning-Operation-Maintenance-Europe-Asia/723. (Accessed 4 March 2025).
[61] Aermec WFGI - Water cooled heat pump reversible water side n.d. https://www.aermec.com/download/?id=16653. (Accessed 4 March 2025).
[62] Clivet - serie SCREWLine4-i WDAT-iK4 120.1 580.2 n.d. https://riclima.ch/wp-content/uploads/2020/01/WDAT-R1234Ze.pdf. (Accessed 4 March 2025).
[63] Decreto Ministeriale 26/06/2015 - Allegato 1 Criteri Generali E Requisiti Delle Prestazioni Energetiche Degli Edifici. n.d.
[64] U.S. Environmental Protection Agency. Emission factors for greenhouse gas inventories n.d. https://www.epa.gov/sites/default/files/2020-04/documents/ghg-emission-factors-hub.pdf (accessed November 17, 2024).
[65] European Environment Agency. Greenhouse gas emission intensity of electricity generation, country leve n.d. https://www.eea.europa.eu/en/analysis/indicators/greenhouse-gas-emission-intensity-of-1/greenhouse-gas-emission-intensity-of-electricity-generation-country-level (accessed November 17, 2024).